Available online at www.sciencedirect.com
ScienceDirect
Trans. Nonferrous Met. Soc. China 24(2014) 3979−3986
Transactions of Nonferrous Metals Society of China
www.tnmsc.cn

Dechromization and dealumination kinetics in process of Na_2CO_3-roasting pretreatment of laterite ores

Qiang GUO[1,2], Jing-kui QU[1,2], Bing-bing HAN[1,2], Guang-ye WEI[1,2], Pei-yu ZHANG[1,2], Tao QI [1,2]

1. National Engineering Laboratory for Hydrometallurgical Cleaner Production Technology, Beijing 100190, China;
2. Key Laboratory of Green Process and Engineering, Institute of Process Engineering, Chinese Academy of Sciences, Beijing 100190, China

Received 22 January 2014; accepted 6 June 2014

Abstract: A novel process was proposed for the activation pretreatment of limonitic laterite ores by Na_2CO_3 roasting. Dechromization and dealumination kinetics of the laterite ores and the effect of particle size, Na_2CO_3-ore mass ratio, and roasting temperature on Cr and Al extraction were studied. Experimental results indicate that the extraction rates of Cr and Al are up to 99% and 82%, respectively, under the optimal particle size of 44–74 μm, Na_2CO_3-to-ore mass ratio of 0.6:1, and temperature of 1000 °C. Dechromization within the range of 600–800 ºC is controlled by the diffusion through the product layer with an apparent activation energy of 3.9 kJ/mol, and that it is controlled by the chemical reaction at the surface within the range of 900–1100 °C with an apparent activation energy of 54.3 kJ/mol. Besides, the Avrami diffusion controlled model with on apparent activation energy of 16.4 kJ/mol is most applicable for dealumination. Furthermore, 96.8% Ni and 95.6% Co could be extracted from the alkali-roasting residues in the subsequent pressure acid leaching process.

Key words: dechromization; dealumination; kinetics; Na_2CO_3-roasting pretreatment; laterite ore; nickel; cobalt

1 Introduction

The superior properties of Ni lead to an increased demand for the metal, which results in the depletion of the easily extractable Ni sulfide deposits. This has also prompted the mining industry to develop extraction technologies for lateritic Ni [1]. Of all the land Ni reserves, 30% exists as sulfide ores with the balance comprised of oxide ores [2]. The oxide ores account for about 40% of the world's Ni production [3]. Lateritic Ni deposits occur as a result of prolonged chemical weathering of ultramafic rocks containing high proportions of Fe (III) oxide [4] and minor amounts of Ni, Co, Cr and Al [5]. Laterites are mainly divided into two types, i.e., limonitic laterite ores and silicon-magnesium ores. The primary mineral in the limonitic laterite ores is α-FeOOH [6] which forms needle-shaped particles rich in Ni [7].

It is impossible to physically beneficiate Ni due to the complex mineralogy and heterogeneous nature of limonitic laterite ores. In addition, Ni extraction from these ores by traditional pyro- and hydro-metallurgical technologies is costly because of their low Ni content [8−10]. Traditional metallurgical technologies include pyrometallurgical refining [11,12], reduction roasting-ammoniacal ammonium carbonate leaching [13], high-pressure acid leaching (HPAL) [14,15], and so on. Recently, the HPAL technology for processing limonitic laterite ores has become research and industrial application hotspots in hydrometallurgy. However, when this technology was used to treat limonitic laterite ores from Indonesia, the leaching rates of Ni and Co were both low, because some of the Ni and Co were embedded in the chromite or other minerals in the laterite ores [16]. Furthermore, large quantities of acid leach residues with impurities have become unexploited resources that are a serious burden to the environment. Thus, research has been carried out to recover hematite from the acid leach residues mainly containing hematite, quartz, gibbsite and

Foundation item: Project (51125018) supported by the National Natural Science Foundation for Distinguished Young Scholars of China; Project (51204153) supported by the National Natural Science Foundation of China; Project (2011BAC06B07) supported by the National High Technology Research and Development Program, China
Corresponding author: Tao QI, Tel: + 86-10-62631710; E-mail: tqgreen@home.ipe.ac.cn
DOI: 10.1016/S1003-6326(14)63559-7

chromite and upgrade of the residues to a saleable Fe concentrate [17].

Keeping in mind the above situation, a new extraction technology called the alkali roasting–acid leaching (ARAL) process was developed by our research group to process limonitic laterite ores from Indonesia [18]. The general process flow of the ARAL technology is shown in Fig. 1. This technology comprehensively extracts all the valuable components of limonitic laterite ores. There are three advantages of the ARAL technology as follows [16]. First, it comprehensively extracts all the valuable components of limonitic laterite ores, and reduces costs by operating at milder acid leaching conditions and by recycling the alkali and acid media. Second, alkali-roasting activation pretreatment breaks the mineral lattices of laterites, exposing their Ni and Co, which leads to higher extraction of these two metals under milder operation conditions in the subsequent pressure acid leaching process. Lastly, the grade of pressure acid leaching iron residues is increased due to the removal of some impurities (such as Cr and Al) during the pretreatment, which makes iron-making easier.

The purpose of the present work is to obtain essential information on the effect of particle size, Na_2CO_3-to-ore mass ratio, and roasting temperature on Cr and Al extraction by Na_2CO_3 roasting and then leaching with water. Moreover, the dechromization and dealumination kinetics are also investigated in the present work.

2 Experimental

2.1 Materials

The limonitic laterite ores used in the present work were collected from Indonesia. Indonesia is estimated to have this type of laterite ore reserves of around 150 million. The results of the typical composition analysis by inductively coupled plasma-optical emission spectrometry (ICP-OES, Optima 5300DV, PerkinElmer, USA) are presented in Table 1. The mineralogical analysis of the samples by XRD (Philips 1140, Cu K_α, 40 mA current, 30 kV) indicates that the major crystalline mineral of the laterite ores is goethite, with minor amounts of hematite, magnetite, chromite, gibbsite, and manganite (see Fig. 2). The laterite ores are collected for SEM observation (Electron Corporation, JSM−6700F), as shown in Fig. 3. Goethite, presenting a stalactitic shape, is the major Ni-bearing mineral. Spheroidal particles are mainly Ni oxide grains that are rich in the goethite lattice. Water for the experiment and analysis was purified using a water super-purification machine (Milli-Q, Millipore). The solid Na_2CO_3 was of reagent grade (Beijing Chemical Plant).

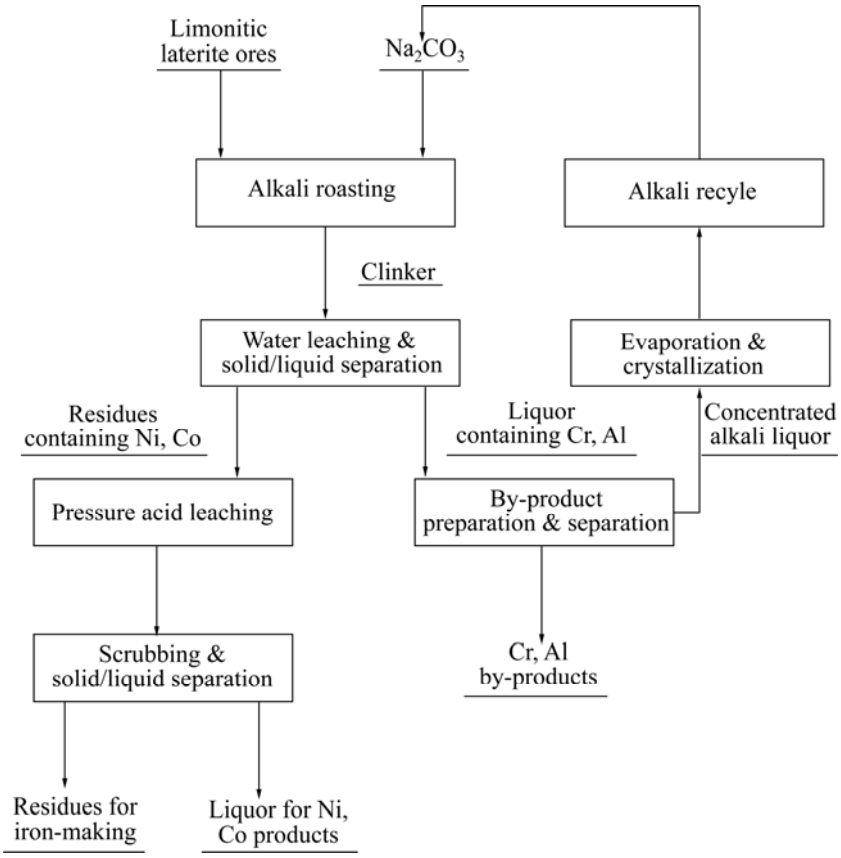

Fig. 1 General process flow sheet of ARAL technology for processing laterite ores from Indonesia

Table 1 Composition analysis results of limonitic laterite samples from Indonesia (mass fraction, %)

Fe	Ni	Co	Cr_2O_3	Al_2O_3	MgO	SiO_2	Mn
47.04	0.55	0.037	5.01	7.68	0.50	1.53	0.34

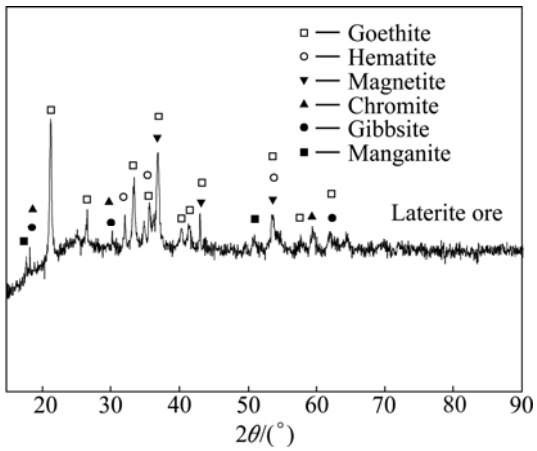

Fig. 2 XRD pattern of laterite samples from Indonesia

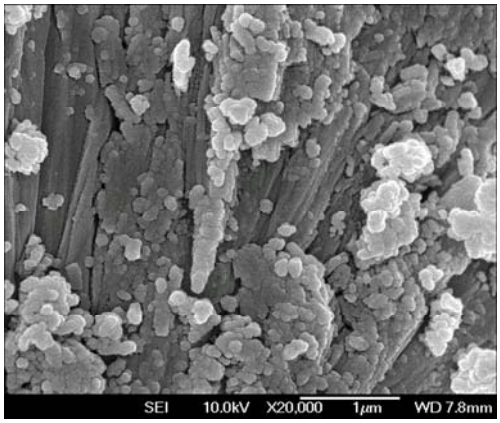

Fig. 3 SEM image of laterite samples from Indonesia

2.2 Experimental equipment and procedures

The laterite samples were dried, ground, and dry-sieved to various narrow-range fractions. The alkali-roasting tests were performed in a muffle furnace using corundum crucibles with the temperature of the muffle furnace controlled using a programmable temperature controller with a precision of ±1 °C. The calculated Na_2CO_3 and laterite samples according to a certain Na_2CO_3-to-ore mass ratio were homogeneously mixed in the corundum crucibles and then placed into the muffle furnace and heated to a preset temperature for a required time with free access of air.

The Na_2CO_3-roasting reaction could be described as follows:

$$Na_2CO_3=Na_2O+CO_2 \quad (1)$$

$$Na_2O+1/2Cr_2O_3+3/4O_2=Na_2CrO_4 \quad (2)$$

$$Na_2O+1/2FeO\cdot Cr_2O_3+7/8O_2=Na_2CrO_4+1/4Fe_2O_3 \quad (3)$$

$$Na_2O+Al_2O_3=2NaAlO_2 \quad (4)$$

$$Na_2O+SiO_2=Na_2SiO_3 \quad (5)$$

$$2NaAlO_2+nNa_2SiO_3=Na_2O\cdot Al_2O_3\cdot nSiO_2+nNa_2O \quad (6)$$

To calculate the degree of Cr and Al extraction, the molten product was removed rapidly at selected time intervals during a run and then cooled at room temperature. The cooled alkali-roasting clinker was ground and then put into glass beakers with water to form a slurry with liquid-to-solid mass ratio of 2:1. The beakers were placed in an electrical heating oil-bath vessel equipped with a continuous agitating device, and leached with water at 90 °C. After complete leaching with water, the slurry was separated by Buchner funnel into filtrate rich in Cr, Al and filter cake rich in Ni, Co, and Fe. The filter cake was dried and then dissolved in diluted HCl solution and analyzed for its Cr and Al content by ICP-OES. Leaching was calculated using the following formula:

$$X=100-(V\times\rho)/(m_i/m_l\times m_p\times w)\times 100 \quad (7)$$

where X is the fractional conversion of impurity (Cr or Al); ρ is the impurity concentration in the HCl solution (measured by ICP-OES) after dissolution of the filter cake; m_l and m_i are the total mass of the filter cake and laterite samples, respectively; m_p is the mass of the filter cake dissolved in HCl solution; w is the mass fraction of metal in the laterite sample; V is the volume of HCl solution used.

3 Results and discussion

3.1 Effect of particle size

The dependence of the particle size on Cr and Al extraction was investigated by alkali roasting at 1000 °C and a Na_2CO_3-to-ore mass ratio of 0.6:1, using the three particle size fractions of the laterite samples, namely, 100−125, 74−100, and 44−74 μm. The results presented in Figs. 4 and 5 show that Cr and Al extraction both increase with the decrease in the particle size. This indicates

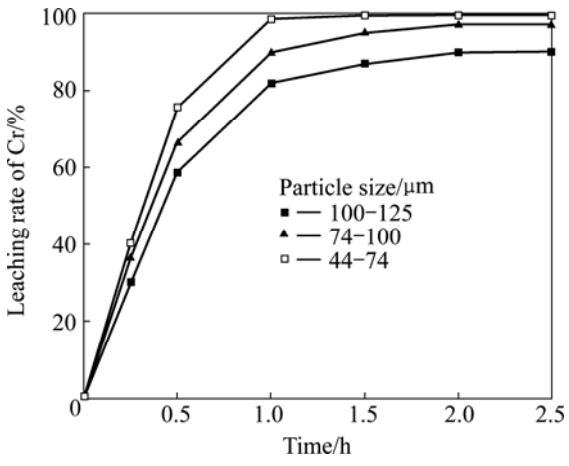

Fig. 4 Effect of particle size on leaching rate of Cr

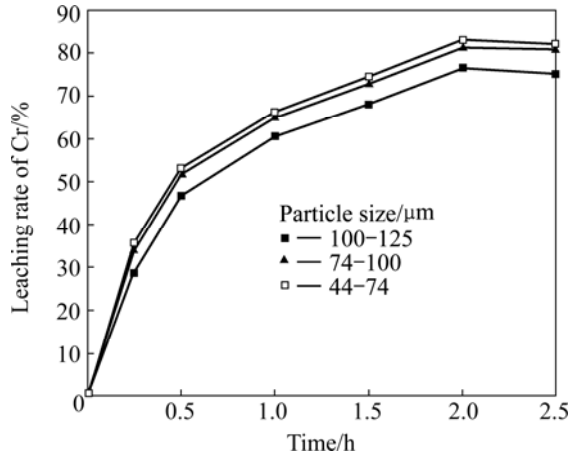

Fig. 5 Effect of particle size on leaching rate of Al

that decreasing the clinker size increases the specific surface and its reactivity. Thus, subsequent experiments were performed using laterite sample fractions of 44–74 μm particle size.

3.2 Effect of Na_2CO_3-to-ore mass ratio

Na_2CO_3 acts as a fluxing agent in the reaction mixture. Excess Na_2CO_3 is necessary to ensure sufficient extent of reaction. This amount of Na_2CO_3 does not significantly affect the economy of the whole process because of the recycling procedure in the overall process.

The influence of the 0.4−0.8 Na_2CO_3-to-ore mass ratio on the leaching rates of Cr and Al at 1000 °C was investigated. As shown in Fig. 6, the leaching of Cr improves with an increase in the Na_2CO_3-to-ore mass ratio from 0.4:1 to 0.8:1, whereas little increase occurs between the ratios 0.8:1 and 0.6:1. The extent of leaching considerably increases at the initial stages of roasting and stabilizes after 1 h. Besides, it can be seen from Fig. 7 that the leaching rate of Al also improves with an increase in the Na_2CO_3-to-ore mass ratio, whereas little decrease occurs with the extended roasting time, mainly due to the generation of sodium aluminosilicate

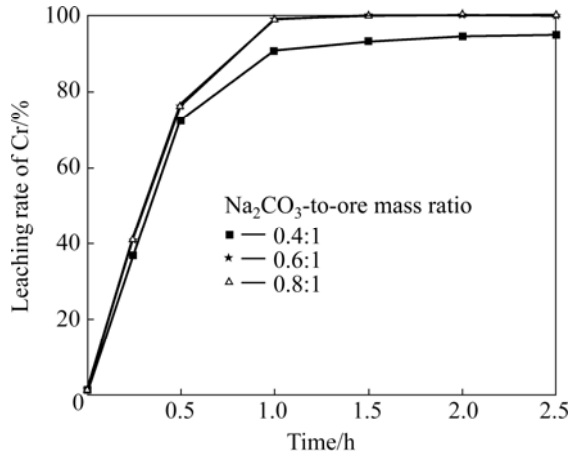

Fig. 6 Effect of Na_2CO_3 to-ore mass ratio on leaching rate of Cr

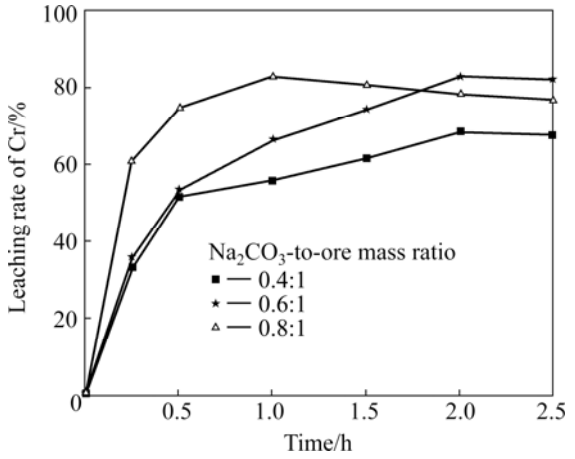

Fig. 7 Effect of Na_2CO_3-to-ore mass ratio on leaching rate of Al

($Na_2O{\cdot}Al_2O_3{\cdot}nSiO_2$) [16]. The optimal ratio is found to be 0.6:1, at which leaching rates up to 99% and 82% for Cr and Al can be obtained, respectively.

3.3 Effect of roasting temperature

The roasting temperature dependence of the alkali-roasting process can be used to estimate the apparent free energy and elucidate the macro-kinetics of the process. The influence of roasting temperature on the leaching rates of Cr and Al was examined at 600−1100 °C and a Na_2CO_3-to-ore mass ratio of 0.6:1. The results in Figs. 8 and 9 show that the leaching rates of Cr and Al both increase with the increase in roasting temperature from 600 to 1000 °C, whereas considerable decrease for Al occurs at 1100 °C. Results of SEM observation of alkali-roasting residues at 1100 °C (see Fig. 10) indicate that increasing temperature leads to serious sintering of the residues, which results in a lower leaching rate of Al during the water leaching process. The other reason could be attributed to the fact that Na_2CO_3 reacts with the silicate compounds in the laterite ores to form Na_2SiO_3 (reaction (5)), and then with the

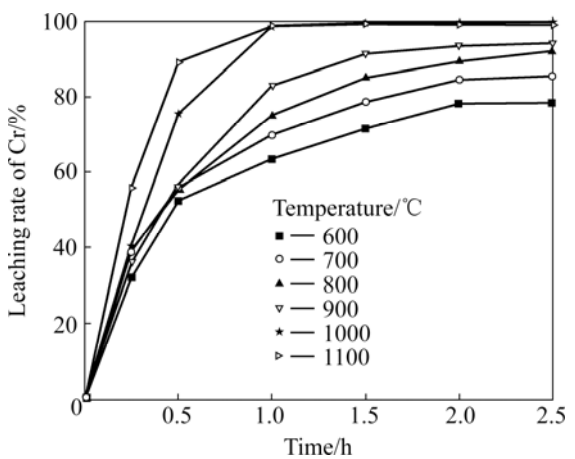

Fig. 8 Effect of roasting temperature on leaching rate of Cr

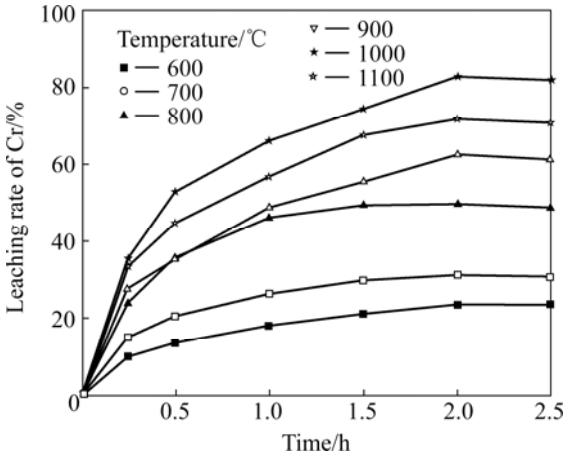

Fig. 9 Effect of roasting temperature on leaching rate of Al

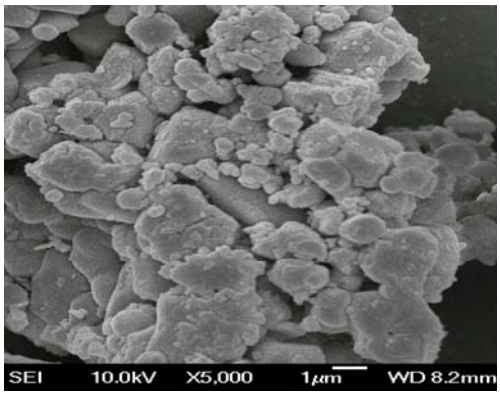

Fig. 10 SEM image of Na_2CO_3-roasting residues of laterite ores

continued increase in roasting temperature, it subsequently reacts with $NaAlO_2$ to form an insoluble complex called $Na_2O{\cdot}Al_2O_3{\cdot}nSiO_2$ precipitate (reaction (6)), which results in a loss of soluble Al. Consequently, 1000 °C is the favorable roasting temperature for the leaching of Cr and Al.

3.4 Dechromization kinetics

Activation pretreatment of limonitic laterite ores by Na_2CO_3 roasting at 600–1100 ºC is a heterogeneous liquid–solid reaction process that could be analyzed with the shrinking-core model [19]. Assuming ideal conditions, the reaction rate of dechromization may be controlled by one of the following steps: diffusion through the boundary or product layers, and the chemical reaction on the surface. Assuming that the particles of laterites have spherical geometry, the following kinetic equations apply for different rate-controlling steps.

Boundary layer diffusion-controlled process:

$$x=k_1t \tag{8}$$

Product layer diffusion-controlled process:

$$[1-(1-x)^{1/3}]^2=k_2t \tag{9}$$

Chemical reaction-controlled process:

$$1-(1-x)^{1/3}=k_3t \tag{10}$$

where x is the Cr fraction reacted at time t; k_1, k_2 and k_3 are the apparent rate constants of Eqs. (8)−(10), respectively.

3.4.1 Diffusion-controlled process

Based on the Cr fractional conversion x at time t given in Fig. 8, x, $[1-(1-x)^{1/3}]^2$, and $1-(1-x)^{1/3}$ were calculated and subsequently plotted against reaction time t, according to Eqs. (8)−(10). The results show that the diffusion-controlled model is suitable for the leaching of Cr within the range of 600−800 °C. The rate constants (k) and correlation coefficients (R^2) for the diffusion-controlled model are listed in Table 2. Furthermore, plots of $[1-(1-x)^{1/3}]^2$ versus t (see Fig. 11) indicate that the leaching rate of Cr at 600–800 °C within 2 h has good correlation with the diffusion-controlled kinetics derived from Eq. (9). The apparent rate constant was determined from the straight lines of Fig. 11, and plotted according to the Arrhenius equation, as shown in Fig. 12. The calculated apparent activation energy is found to be 3.9 kJ/mol. The activation energy of a diffusion-controlled process is usually less than 20 kJ/mol [20]. Research results by CHANDRA et al indicated that melting oxidization of chromite at 600−650 °C was controlled by the diffusion through the product layer with an apparent activation energy of 61.49 kJ/mol [21]. The above results confirm that dechromization within the range of 600−800 °C is controlled by diffusion through the product layer.

Table 2 Rate constants and correlation coefficients for diffusion-controlled model

θ/℃	$T^{-1}/10^{-3}K^{-1}$	k	ln$k$	R^2
600	1.145	0.07924	−2.535	0.993
700	1.028	0.10818	−2.224	0.999
800	0.932	0.14603	−1.978	0.994

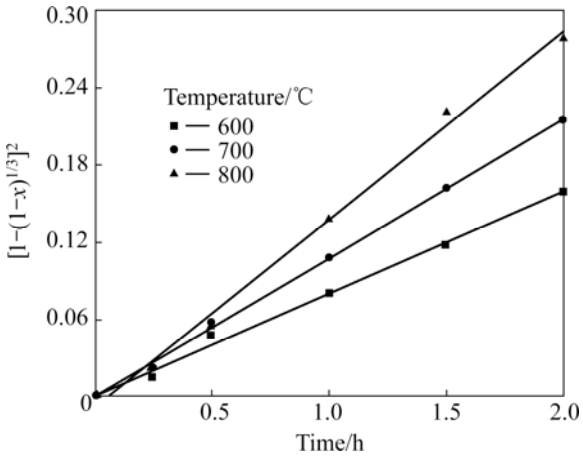

Fig. 11 Plots of $[1-(1-x)^{1/3}]^2$ vs time

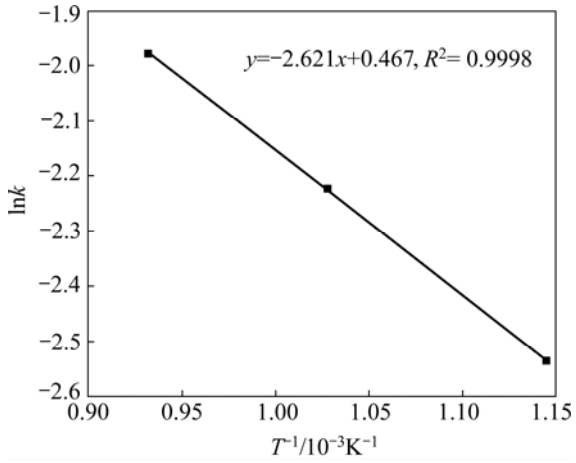

Fig. 12 Arrhenius plot for leaching rate of Cr from laterite ores at 600−800 °C

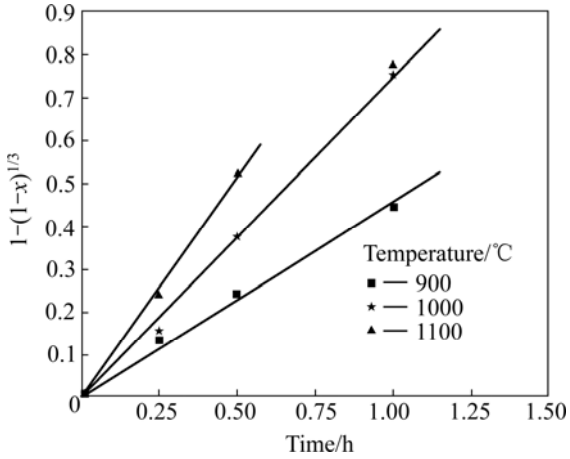

Fig. 13 Plots of $1-(1-x)^{1/3}$ vs time

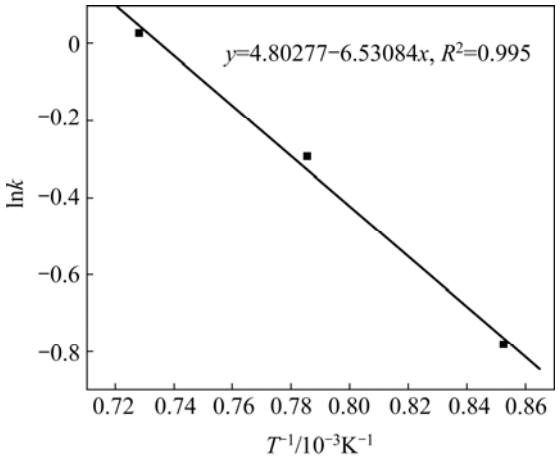

Fig. 14 Arrhenius plot for leaching rate of Cr from laterite ores at 900−1100 °C

3.4.2 Chemical-reaction controlled process

Besides, the calculated results show that the chemical reaction-controlled model is suitable for the leaching of Cr within the range of 900−1100 °C. The rate constants (k) and correlation coefficients (R^2) for the surface chemical reaction-controlled model are listed in Table 3. Furthermore, plots of $1-(1-x)^{1/3}$ versus t (see Fig. 13) indicate that the leaching of Cr at 900–1100 °C within 1 h has good correlation with the chemical reaction-controlled kinetics derived from Eq. (10). The apparent rate constant was determined from the straight lines of Fig. 13, and plotted according to the Arrhenius equation, as shown in Fig. 14. The calculated apparent activation energy is found to be 54.3 kJ/mol. The activation energy of a chemically controlled process is usually greater than 41.8 kJ/mol [22]. Traditional oxidization roasting of chromite using Na_2CO_3 within the range of 900−1100 °C is controlled by the chemical reaction on the surface with an apparent activation energy of 75.36−142.35 kJ/mol [23]. Research results by LI et al [24] indicated that oxidization roasting of chromite within the range of 950−1100 °C was controlled by the chemical reaction on the surface with an apparent activation energy of 68.7 kJ/mol. The above results confirm that dechromization within the range of 900−1100 °C is controlled by the chemical reaction on the surface.

Consequently, Cr extraction from the laterite ores is a diffusion-controlled process within the range of 600−800 °C and a chemical reaction-controlled process within the range of 900–1100 °C, respectively.

Table 3 Rate constants and correlation coefficients for chemical reaction-controlled model

θ/℃	$T^{-1}/10^{-3}K^{-1}$	k	ln k	R^2
900	0.853	0.45809	−0.7807	0.998
1000	0.786	0.74629	−0.2926	0.999
1100	0.728	1.02809	0.0277	0.999

3.5 Dealumination kinetics

Based on the Al fractional conversion x at time t given in Fig. 9, the kinetic Eqs. (8)−(10) are not suitable for the leaching of Al within the range of 600−1100 °C. Therefore, it is assumed that the Al extraction applies for the Avrami diffusion controlled model:

$$\ln[-\ln(1-x)]=\ln k_4+n\ln t \quad (11)$$

where x is the Al fraction reacted at time t, and k_4 is the apparent rate constants of Eq. (11).

The results show that the Avrami diffusion-controlled model is suitable for the leaching of Al within the range of 600−1100 °C. The rate constants (k) and correlation coefficients (R^2) for the Avrami diffusion-controlled model are listed in Table 4. Furthermore, plots of $\ln[-\ln(1-x)]$ versus $\ln t$ (see Fig. 15) indicate that the leaching of Al at 600–1100 °C has good correlation with the Avrami diffusion-controlled kinetics derived from

Eq. (11). Therefore, Al extraction from the laterite ores is an Avrami diffusion-controlled process at the Na_2CO_3-to-ore mass ratio of 0.6:1. The apparent rate constant was determined from the straight lines of Fig. 15, and plotted according to the Arrhenius equation, as shown in Fig. 16. The calculated apparent activation energy is found to be 16.4 kJ/mol. Research results by XIAO et al [25] indicated that the leaching process of bauxite sintering clinker was controlled by the internal diffusion with an apparent activation energy of 11.77 kJ/mol, which are similar to the results reported in this work.

Table 4 Correlation coefficients of $\ln[-\ln(1-x)]$ vs $\ln t$ at different temperatures

θ/℃	Equation	R^2
600	$\ln[-\ln(1-x)]=-3.22467+0.4062\ln t$	0.999
700	$\ln[-\ln(1-x)]=-2.93802+0.4299\ln t$	0.993
800	$\ln[-\ln(1-x)]=-2.81736+0.57845\ln t$	0.99
900	$\ln[-\ln(1-x)]=-2.64138+0.54912\ln t$	0.993
1000	$\ln[-\ln(1-x)]=-2.5098+0.63684\ln t$	0.99
1100	$\ln[-\ln(1-x)]=-2.37218+0.54663\ln t$	0.996

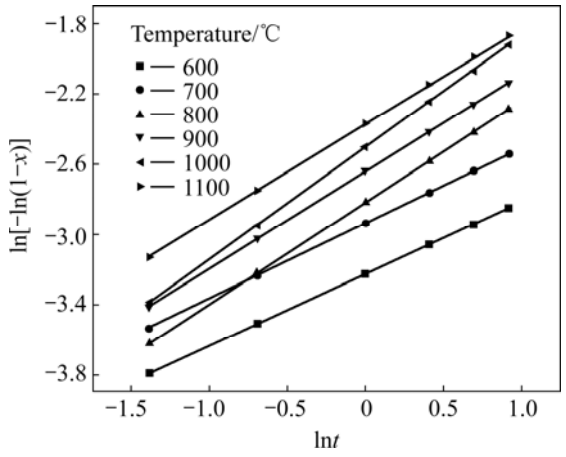

Fig. 15 Plots of $\ln[-\ln(1-x)]$ vs $\ln t$

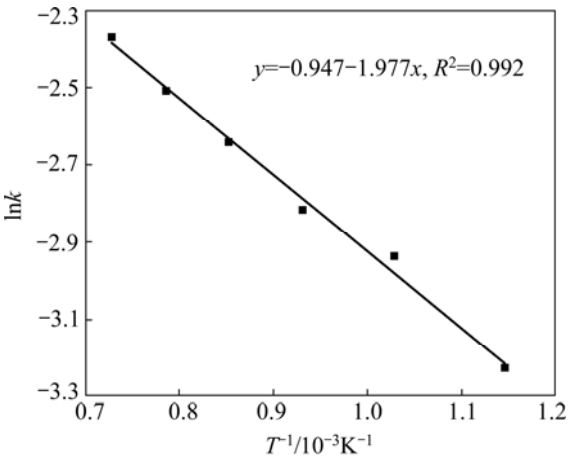

Fig. 16 Arrhenius plot of $\ln k$ vs $1/T$

3.6 Experiments on leaching of Ni and Co by pressure acid leaching

The subsequent pressure acid leaching experiments of the residues pretreated with alkali roasting were performed to evaluate the effect of pretreatment on the leaching of Ni and Co and the grade of acid leach iron residues.

The pressure acid leaching experiments were carried out under a liquid-to-solid mass ratio of 3.5:1, free acid concentration of 50 g/L, leaching temperature of 200 °C, leaching time of 1.5 h, and leaching pressure of 1.6 MPa. The experimental results show that the leaching rates of Ni and Co from the water leach residues of the alkali-roasting clinker are 96.8% and 95.6%, respectively, in the subsequent pressure acid leaching process. The pressure acid leaching operation conditions of the ARAL technique for processing limonitic laterite ores are milder compared with those of traditional HPAL (250−270 °C, 5−6 MPa). This is because alkali-roasting activation pretreatment breaks the mineral lattices of the laterite, which makes Ni and Co more exposed and then easily leached. Meanwhile, the grade of acid leach iron residues can reach 62.33% due to the removal of impurities in the laterite ores by the alkali-roasting pretreatment.

4 Conclusions

1) The experimental results on activation pretreatment of laterite ores by Na_2CO_3 roasting indicate that increasing the Na_2CO_3-to-ore mass ratio and roasting temperature, and decreasing the particle size increase Cr and Al extraction rates. Approximately 99% Cr and 82% Al in the laterite ores can be extracted under the optimal temperature of 1000 °C, Na_2CO_3-to-ore mass ratio of 0.6:1, and particle of size of 44−74 μm.

2) The results on dechromization kinetics indicate that dechromization within the range of 600–800 ºC is controlled by the diffusion process with an apparent activation energy of 3.9 kJ/mol, and that it is controlled by the chemical reaction process within the range of 900–1100 °C with an apparent activation energy of 54.3 kJ/mol.

3) The results on dealumination kinetics indicate that dealumination within the range of 600−1100 °C is controlled by the Avrami diffusion model with an apparent activation energy of 16.4 kJ/mol.

4) 96.8% Ni and 95.6% Co can be extracted from the alkali-roasting residues in the subsequent pressure acid leaching process. Meanwhile, the grade of acid leach iron residues can reach 62.33%. The iron residues with low Cr content are more suitable raw materials for iron making.

References

[1] LANDERS M, GILKES R J, WELLS M. Dissolution kinetics of dehydroxylated nickeliferous goethite from limonitic lateritic nickel ore [J]. Applied Clay Science, 2009, 42: 615−624.

[2] ZHU D Q, CUI Y, HAPUGODA S, VINING K, PAN J. Minerology and crystal chemistry of a low grade nickel laterite ore [J]. Transactions of Nonferrous Metals Society of China, 2012, 22(4): 907−916.

[3] GLEESON S A, HERRINGTON R J, DURANGO J, VELAZQUZE C A, KOLL G. The mineralogy and geochemistry of de Cerro Matoso S. A. Ni laterite deposit, Montelíbano, Colombia [J]. Economic Geology, 2004, 99: 1197−1213.

[4] WANG Cheng-yan, YIN Fei, CHEN Yong-qiang, WANG Zhong, WANG Jun. Worldwide processing technologies and progress of nickel laterites [J]. The Chinese Journal of Nonferrous Metals, 2008, 18: s1−s8. (in Chinese)

[5] OLANIPEKUN E O. Kinetics of leaching laterite [J]. International Journal of Mineral Processing, 2000, 60(1): 9−14.

[6] PICKLES C A. Microwave heating behaviour of nickeliferous limonitic laterite ores [J]. Minerals Engineering, 2004, 17(6): 775−784.

[7] GEORGIOU D, PAPANGELAKIS V G. Characterization of limonitic laterite and solid during sulfuric acid pressure leaching using transmission electron microscopy [J]. Minerals Engineering, 2004, 17(3): 461−463.

[8] BRAND N W, BUTT C R M, ELIAS M. Nickel laterites: Classification and features [J]. AGSO Journal of Australian Geology and Geophysics, 1998, 17(4): 81−88.

[9] SWAMY Y V, KAR B B, MOHANTY J K. Physico-chemical characterization and sulphatization roasting of low-grade nickeliferous laterites [J]. Hydrometallurgy, 2003, 69(1−3): 89−98.

[10] DEEPATANA A, TANG J A, VALIX M. Comparative study of chelating ion exchange resins for metal recovery from bioleaching of nickel laterite ores [J]. Minerals Engineering, 2006, 19(12): 1280−1289.

[11] KOTZE I J. Pilot plant production of ferronickel from nickel oxide ores and dusts in a DC arc furnace [J]. Minerals Engineering, 2002, 15(11): 1017−1022.

[12] LI Yan-jun, SUN Yong-sheng, HAN Yue-xin, GAO Peng. Coal-based reduction mechanism of low-grade laterite ore [J]. Transactions of Nonferrous Metals Society of China, 2013, 23(11): 3428−3433.

[13] O'CONNOR F, CHEUNG W H, VALIX M. Reduction roasting of limonite ores: Effect of dehydroxylation [J]. International Journal of Mineral Processing, 2006, 80(2−4): 88−99.

[14] WHITTINGTON B I, MCDONALD R G, JOHNSON J A, MUIR D M. Pressure acid leaching of Bulong nickel laterite ore: Part I. Effect of water quality [J]. Hydrometallurgy, 2003, 70(1−3): 31−46.

[15] GAO Xue-yi, SHI Wen-tang, LI Dong, TIAN Qing-hua. Leaching behavior of metals from limonitic laterite ore by high pressure acid leaching [J]. Transactions of Nonferrous Metals Society of China, 2011, 21(1): 191−195.

[16] GUO Qiang, QU Jing-kui, QI Tao, WEI Guang-ye, HAN Bing-bing. Activation pretreatment of limonitic laterite ores by alkali-roasting method using sodium carbonate [J]. Minerals Engineering, 2011, 24(8): 825−832.

[17] STAMBOLIADIS E, ALEVIZOS G, ZAFIRATOS J. Leaching residue of nickeliferous laterites as a source of iron concentrate [J]. Minerals Engineering, 2004, 17: 245−252.

[18] DONG Shu-tong, WANG Cheng-yan, QI Tao, QU Jing-ui, ZHAO Ping, YIN Fei. A treatment processing for the limonitic nickeliferous laterite ores by alkali-acid circulation: China, 0910180397.6 [P] 2009−10−27. (in Chinese)

[19] MU Wen-ning, ZHAI Yu-chun. Desiliconization kinetics of nickeliferous laterite ores in molten sodium hydroxide system [J]. Transactions of Nonferrous Metals Society of China, 2010, 20(2): 330−335.

[20] ZHENG Shi-li. Basic research and optimization on liquid phase oxidation process in chromate clean production technology [D]. Beijing: Institute of Process Engineering, Chinese Academy of Sciences, 2000: 36−37. (in Chinese).

[21] CHANDRA D, MAGEE C B, LEFFLER L. Extraction of chromium from low-grade chromium-bearing ores [R]. Denver: Denver Research Inst, CO, 1982: PB83−106781.

[22] LUO Wei, FENG Qi-ming, QU Le-ming, ZHANG Guo-fan, CHEN Yun. Kinetics of saprolitic laterite leaching by sulphuric acid at atmospheric pressure [J]. Minerals Engineering, 2010, 23(6): 458−462.

[23] DI Yi, JI Zhu. Production and application of chromium compounds [M]. Beijing: Chemical Industry Press, 2003: 52−56. (in Chinese)

[24] LI Xiao-bin, QI Tian-gui, PENG Zhi-hong, LIU Gui-hua, ZHOU Qiu-sheng. Kinetics of chromite ore in oxidation roasting process [J]. The Chinese Journal of Nonferrous Metals, 2010, 20(9): 1822−1828. (in Chinese)

[25] XIAO Wei, LI Wei, ZHANG Nian-bing, LI Zhi-ying. Leaching kinetics of calcium aluminate sinter [J]. Light Metals, 2009, 8: 23−27. (in Chinese)

碳酸钠焙烧预处理红土镍矿过程除铬和铝动力学

郭 强[1,2]，曲景奎[1,2]，韩冰冰[1,2]，魏广叶[1,2]，张培育[1,2]，齐 涛[1,2]

1. 湿法冶金清洁生产技术国家工程实验室，北京 100190；

2. 中国科学院 过程工程研究所，绿色过程与工程院重点实验室，北京 100190

摘 要：开发碳酸钠碱熔焙烧预处理红土镍矿的新工艺，对红土镍矿碱熔脱除铬和铝动力学以及矿石粒度和碱矿质量比、焙烧温度等影响铬和铝浸出率的因素进行系统研究。结果表明：在矿石粒度为 44~74 μm、碱矿质量比为 0.6:1 和焙烧温度为 1000 °C 的条件下，铬和铝的浸出率分别达到 99%和 82%以上。在 600−800 °C 温度范围内，除铬反应受产物层扩散控制，其表观活化能为 3.9 kJ/mol；在 900~1100 °C 温度范围内，除铬反应受表面化学反应控制，其表观活化能为 54.3 kJ/mol。此外，在 600~1100 °C 温度范围内，除铝反应受 Avrami 内扩散控制，其表观活化能为 16.4 kJ/mol。在后续对碱熔渣进行加压酸浸过程中，镍和钴的浸出率分别达到 96.8%和 95.6%。

关键词：除铬；除铝；动力学；碳酸钠焙烧预处理；红土镍矿；镍；钴 **(Edited by Yun-bin HE)**